Journal of Drug Targeting

http://informahealthcare.com/drt
ISSN: 1061-186X (print), 1029-2330 (electronic)

J Drug Target, 2013; 21(10): 994–1000
 DOI: 10.3109/1061186X.2013.840639

informa healthcare

ORIGINAL ARTICLE

Anti-cancer activity of anti-GLUT1 antibody-targeted polymeric micelles co-loaded with curcumin and doxorubicin

Abraham H. Abouzeid[1], Niravkumar R. Patel[1], Ilya M. Rachman[2], Sean Senn[2], and Vladimir P. Torchilin[1]

[1]*Department of Pharmaceutical Sciences, Center for Pharmaceutical Biotechnology and Nanomedicine, Northeastern University, Boston, MA, USA and* [2]*Immix Biopharma LLC, Los Angeles, CA, USA*

Abstract

Background: Treatment of late stage cancers has proven to be a very difficult task. Targeted therapy and combinatory drug administration may be the solution.
Purpose: The study was performed to evaluate the therapeutic efficacy of PEG-PE micelles, co-loaded with curcumin (CUR) and doxorubicin (DOX), and targeted with anti-GLUT1 antibody (GLUT1) against HCT-116 human colorectal adenocarcinoma cells both *in vitro* and *in vivo*.
Methods: HCT-116 cells were treated with non-targeted and GLUT1-targeted CUR and DOX micelles as a single agent or in combination. Cells were inoculated in female nude mice. Established tumors were treated with the micellar formulations at a dose of 4 mg/kg CUR and 0.4 mg/kg DOX every 2 d for a total of 7 injections.
Results: CUR + DOX-loaded micelles decorated with GLUT1 had a robust killing effect even at low doses of DOX *in vitro*. At the doses chosen, non-targeted CUR and CUR + DOX micelles did not exhibit any significant tumor inhibition versus control. However, GLUT1-CUR and GLUT1-CUR + DOX micelles showed a significant tumor inhibition effect with an improvement in survival.
Conclusion: We showed a dramatic improvement in efficacy between the non-targeted and GLUT1-targeted formulations both *in vitro* and *in vivo*. Hence, we confirmed that GLUT1-CUR + DOX micelles are effective and deserve further investigation.

Keywords

Antibody-targeted nanoparticles, colorectal carcinoma, drug-resistance, glucose transporters, GLUT-1, nuclear factor-kappa B (NF-κB)

History

Received 16 July 2013
Revised 27 August 2013
Accepted 30 August 2013
Published online 7 October 2013

Introduction

Despite significant improvements in detection and treatment of early stages of cancers, the ability to effectively treat advanced forms of the disease is still hindered by cancer's resistance to chemotherapy, biologics and radiotherapy. Available evidence points to the nuclear factor-kappa B (NF-κB)-induced cascade of gene expression as instrumental in generating chemo- and radiation-resistant tumor phenotypes [1]. Many published studies show a correlation between induction and constitutive overexpression of NF-κB and the resistant tumor phenotype in breast [2], colon [3], pancreas [4] and other tissues. NF-κB upregulates the inhibitory of apoptosis proteins (IAPs) such as COX2, BCL2 and Survivin [5], thus promoting tumor proliferation, invasion and metastasis [6]. Many conventional chemotherapeutic agents, such as doxorubicin (DOX) and paclitaxel (PCL), upregulate NF-κB especially at suboptimal doses [7]. Adding curcumin (CUR) helps blunt this effect. CUR, the principal curcuminoid of the Indian spice turmeric, has shown excellent NF-κB – inhibitory action against many different cancer cell types *in vitro* [8]. CUR downregulates NF-κB mainly by AKT downregulation [5]. Inhibition of NF-κB activation appears to restore cancer cell's sensitivity to chemo- and radiotherapy [9]. The wealth of data supporting CUR's anti-cancer activity led to multiple attempts at its use in human clinical trials. Unfortunately, the delivery of sufficient quantities of CUR to cancer cells *in vivo* remains a major challenge in clinical oncology [10].

Part of the challenge is the directly related to the hydrophobic nature of CUR and its poor oral bioavailability. This limitation maybe also overcomes with an appropriate drug delivery system. For example, Tsai et al. utilized a poly-lactic-co-glycolic acid (PLGA) nano-formulation of CUR to increase the oral bioavailability by 22-fold compared to conventional CUR [11]. Shaikh et al. encapsulated CUR into a biodegradable nanoemulsion that exhibited a 9-fold increase in oral bioavailability when compared to CUR administered [12]. Many other published studies also reported an improvement in the *in vivo* bioavailability of CUR by employing various nanocarrier systems including solid lipid nanoparticles [13,14], PVP capped gold nanoparticles [15], chitosan nanoparticles [16], self-assembling methoxy poly(ethylene glycol)–palmitate nanocarriers [17], nanospheres [18], among many others. In addition to the increased bioavailability of CUR achieved by nanocarriers, utilizing a targeted nanoparticle drug carrier systems provide much higher tumor cell

Address for correspondence: Vladimir P. Torchilin, Distinguished Professor, Department of Pharmaceutical Sciences, Center for Pharmaceutical Biotechnology and Nanomedicine, Northeastern University, 140 The Fenway, Room 211/214, 360 Huntington Ave, Boston, MA 02115, USA. Tel: 617-373-3206. Fax: 617-373-7509. E-mail: V.Torchilin@neu.edu

uptake of their payloads than non-targeted lipid- or polymer-based drug carriers [19]. The present study was designed to test the cancer-inhibitory effect of a micellar nanoparticle system carrying various combinations of CUR and DOX decorated with the anti-GLUT1 antibody (GLUT1) for tumor-targeting.

Glucose is a polar molecule and cannot readily get into cells via simple diffusion. A family of proteins, SLC2/GLUT, regulates glucose uptake into cells. There are 14 GLUT proteins including the GLUT1 protein [20]. Although the GLUT1 glucose transporter is found in normal tissues, it is significantly overexpressed on many types of tumors [21–24] to support cell growth and is thought to contribute significantly to the Warburg effect [25]. Healthy cells normally depend on mitochondrial oxidative phosphorylation to produce enough ATP in order to execute the various cellular processes necessary for subsistence. However, most cancer cells rely on aerobic glycolysis, a phenomenon termed the Warburg effect, in addition to oxidative phosphorylation to generate sufficient energy to maintain survival and growth [26]. Furthermore, GLUT1 forms the basis for tumor visualization by PET scan using FDG-labeled glucose [27,28]. GLUT1 is one of the most studied transporters, and many studies have reported that the overexpression of GLUT1 is a marker of poor prognosis and decrease in survival among variety of cancer types [29–32]. The increased expression of GLUT1 enables rapidly growing cancer cells to acquire enough energy even under hypoxic conditions via the glycolytic pathway. Interestingly, the hypoxia inducible factor (HIF), which is upregulated in many cancers, enhances the expression of GLUT1 and other proteins that are necessary for glycolysis [33]. This increased expression of GLUT1 provides an ideal molecular target for anti-cancer therapeutics.

In this study, we investigated the efficacy of the GLUT1-targeted CUR and DOX-loaded micelles as a novel anti-cancer treatment using a colorectal carcinoma as a model cell type. These CUR/DOX co-loaded polymeric micelles decorated with GLUT1had a robust tumor killing effect both *in vitro* and in nude mouse xenografts.

Materials and methods

Materials

1,2-Distearoyl-sn-glycero-3-phosphoethanolamine-N-[methoxy (polyethylene glycol)-2000] (PEG_{2000}–DSPE) was purchased from CordenPharma International (Plankstadt, Germany); 1,2-dioleoyl-sn-glycero-3-phosphoethanolamine (DOPE) was purchased from Avanti Polar Lipids (Alabaster, AL) and used without further purification; pNP-PEG_{3400}-pNP was purchased from Laysan Bio (Arab, AL). CUR was purchased from Sigma (St. Louis, MO, catalog #C7727). DOX free base was purchased from US Biological (Swampscott, MA). GLUT1 (C-20) sc-1605 antibody was purchased from Santa Cruz Biotechnology, Inc. (Santa Cruz, CA). CellTiter-blue® was purchased from Promega (Madison, WI). Matrigel™ basement membrane matrix was purchased from BD Biosciences (Bedford, MA). All other reagents and buffer solution components were analytical grade preparations.

Methods

Cell cultures

HCT-116 human colon cancer cells (CCL-247™) were purchased from ATCC (Manassas, VA) and maintained in McCoy's 5A medium (ATCC 30-2007™) supplemented with 10% heat-inactivated fetal calf serum and 1% penicillin, streptomycin, and amphotericin from Cell-Gro (Kansas City, MO). Cells were maintained at 37 °C in a humidified incubator with 5% CO_2, and were passaged according to ATCC protocols.

Preparation of drug-loaded micelles

CUR and/or DOX-loaded micelles were prepared by the thin film hydration method. Specific amounts of CUR (from 3 mg/ml in 0.1% acetic acid methanol stock solution) and/or DOX free base (from 0.5 mg/ml in methanol stock solution) were added to PEG_{2000}-PE in chloroform. The concentration of the micelle-forming material used in all experiments was 5 mM. Organic solvents were removed by rotary evaporation, to form a thin film of drug/micelle-forming component mixture, which was further dried under high vacuum overnight to remove all remaining organic solvents (Freezone 4.5 Freeze Dry System Labconco, Kansas City, MO). Drug-loaded micelles are spontaneously formed when the film was resuspended in phosphate buffer saline (PBS) pH 7.4. The mixture was incubated in a water bath at 40 °C for 10 min and then vortexed for at least 5 min to ensure a thorough resuspension of the lipid film. Excess non-incorporated drugs were separated by centrifugation (13 500 *g*) for 5 min followed by filtration through a sterile 0.2 μm syringe filter before characterization (Nalgene, Rochester, NY).

Preparation of the anti-GLUT1-targeted micelles

To attach the GLUT1 antibody to the micelles, a pNP-PEG_{3400}-PE component was synthesized. The activated p-nitrophenylcarbonyl (pNP) group at the distal end of the PEG_{3400}-PE monomer reacts with amino-groups of various ligands yielding a stable urethane (carbamate) bond. Synthesis of this polymer was performed according to standardized in-lab procedures. Briefly, pNP-PEG_{3400}-pNP and DOPE were dissolved in dry chloroform, co-incubated with TEA and then reacted at RT under argon with continuous stirring overnight. Solvents were then removed by rotary evaporation, and films were further dried under vacuum for at least 4 h to remove all residual solvents. The dried films were then rehydrated with 0.001 M HCl (pH 3.0) and separated on a sepharose (CL4B) column. Fractions were collected and analyzed by TLC to identify aliquots containing the pNP-PEG_{3400}-PE product; these fractions were then frozen, lyophilized, weighed and reconstituted with chloroform to appropriate stock concentrations, and stored at −80 °C for further use.

To attach GLUT1 to micelles, the reactive polymer, pNP-PEG_{3400}-PE in chloroform was placed in a round-bottom flask. Chloroform was evaporated under a rotary evaporator to form a thin film. Films were further dried under vacuum overnight to remove any residual solvents, and rehydrated with stock GLUT1 solution in 1X PBS (pH 7.4) at a molar

ratio of pNP-PEG_{3400}-PE:GLUT1 40:1. The pH of the solution was adjusted with 1.0 N NaOH to 8.5 as needed. Reaction time was 4 h at RT to allow sufficient GLUT1 conjugation and complete hydrolysis of unreacted pNP groups at the higher pH. GLUT1-PEG-PE micelles were then dialyzed using a 300 000 MWCO membrane against PBS (pH 7.4) for 1 h followed by another 4 h of dialysis in PBS (pH 7.4) to ensure the complete removal of unconjugated antibody. Targeted combination micelles were prepared by co-incubation of drug-loaded micelles with GLUT1-modified micelles at a ratio of 2 mole% of the reactive polymer, pNP-PEG_{3400}-PE, to PEG_{2000}-PE. Samples were vortexed and allowed to mix for at least 4 h at room temperature.

Conjugation efficiency of GLUT1 antibody was measured using a micro BCA kit (Pierce, Rockford, IL) according to the manufacture's manual. Protein content was determined by comparing GLUT1-micelles to a known concentration of antibody and BCA standards. Signals from GLUT1 antibody samples were normalized with plain micelle samples at the same lipid concentration. In addition, to verify the preservation of the anti-GLUT1 specific activity after the conjugation with PEG_{3400}-PE and incorporation into micelles, a direct ELISA was used. Briefly, ELISA plates were coated with 50 µl of 1 µg/ml solution of the GLUT1 blocking peptide and incubated overnight at 4 °C. The plates were then rinsed with PBS containing 0.05% Tween 20 pH 7.4 (PBS-T) and then incubated for 2 h at 37 °C with 200 µl of PBS-T containing 2 mg/ml casein solution as a blocking buffer to prevent a non-specific binding. The blocking buffer was then removed, and 50 µl serial dilutions of GLUT1-containing micelles and GLUT1 standards were added and incubated for 1 h at 37 °C. The plates were extensively washed with PBS-T, and 50 µl of horseradish peroxidase/donkey anti-goat IgG conjugate diluted 5000:1 was added. After 1 h incubation at 37 °C, the plates were washed thoroughly with PBS-T and bound peroxidase was quantified by adding a 50 µl aliquot of K-blue substrate (Neogen Corp., Lexington, KY) and incubating at room temperature in the dark for 30 min. The intensity of the color developed was analyzed using an ELISA reader at the wavelength of 492 nm (BioTek, Model: EL 800, Winooski, VT) and GEN 5.0 software (Winooski, VT).

Characterization of micelles

Micelle size. The micelle size (hydrodynamic diameter) was measured by the dynamic light scattering (DLS) using a N4 Plus Submicron Particle System (Coulter Corporation, Miami, FL, USA). The micelles were diluted with the deionized water until the concentration providing light scattering intensity was between 5×10^4 and 1×10^6 counts/s. The particle size distribution of all samples was measured in triplicate.

Drug incorporation efficiency. Drug incorporation efficiency was measured by reverse phase HPLC using an Xbridge C_{18} (4.6 mm × 250 mm) column (Waters Corporation, Milford, MA) on a Hitachi Elite LaChrome HPLC equipped with an autosampler (Pleasanton, CA) and diode array detector. A gradient method was used with the mobile phase consisting of acetonitrile, water supplemented with 0.2% TFA, and methanol (Table 1). The flow rate was 1 ml/min. DOX was detected at wavelengths of 254 and 485 nm, while CUR was detected at 420 nm. Sample injection volume was kept constant at 50 µl and the sample run time was 20 min. Concentration of drug was determined by measuring the area under the curve of the corresponding peaks. Standard curves of stock drug solution, dissolved in the mobile phase, were used to determine the concentrations of incorporated drugs in micelles. Ten microliters of drug-loaded micelles were diluted in 990 µl of the mobile phase to disrupt the micelles and release the entrapped drug for detection. All samples were analyzed in triplicate. Separation of peaks for both drugs was achieved with DOX and CUR detected at 5.2 and 14 min, respectively. The standard curves obtained for DOX and CUR from the HPLC method had an R^2 value of 0.999 ($n = 3$). This method was developed to detect DOX and CUR in the same micellar formulation. DOX elutes in the initial stage where the mobile phase is relatively polar, whereas CUR elutes at a stage of the gradient when the mobile phase is less polar.

Table 1. Gradient used in the HPLC method for the simultaneous analysis of DOX and CUR incorporation.

Time (min)	Acetonitrile (% v/v)	Water with 0.2% TFA (% v/v)	Methanol (% v/v)
0	25	50	25
7	25	50	25
8.5	40	40	20
10	60	30	10
11.5	80	20	0
13	100	0	0
16	100	0	0
17	25	50	25
20	25	50	25

Cell viability assays

Viability of cells was measured using the CellTiter Blue® (Promega, Madison, WI) viability assay according to the manufacture's protocol. Briefly, cells were seeded in 96-well plates at a density of 3000 cells/well and grown for 24 h. Then cells were incubated with the various formulations for 48 h in serum complete medium. After 48 h of treatment, the medium was removed and the cells were washed with 200 µl serum complete medium and then incubated with 100 µl medium containing 20 µl CellTiter Blue® reagent. Cell viability was then evaluated after 2 h of incubation by measuring the fluorescence (excitation 530 nm, emission 590 nm) using Synergy HT multi-detection microplate reader (Biotek, Winooski, VT). PBS treated cells were taken as controls to calculate percent cell viability and the treatment was carried out in triplicate.

In vivo *tumor inhibition study*

Six-week-old female NU/NU nude mice were purchased from Charles River Laboratories International Inc. (Needham, MA). HCT 116 cell suspensions (5×10^6 cells/0.2 ml PBS:Matrigel 1:1 v/v) were injected subcutaneously into the right flank of 40 animals. After 15 d, when their tumor volumes reached ~250 mm^3, the animals were randomly divided into six groups (six animals per group) since 4 out of

the 40 mice had relatively smaller tumor size compared to the other mice. Then treatment of mice was initiated on day 15. DOX (0.4 mg/kg) and CUR (4 mg/kg) were injected i.v. every other day for a total of 7 injections. Tumor volume was estimated from measurements in two perpendicular dimensions taken manually with vernier calipers and applying the formula $(L \times W^2)/2$, where L is the longest dimension and W is the dimension perpendicular to L. In survival studies, animals were considered non-viable when the tumors reached 1000 mm^3. For statistical analysis, two methods were used to compare the various treatment groups. One way ANOVA was performed from day 0 (time at first injection) to 26 with Tukey's post-test. Two way ANOVA was also performed to determine significance between the various treatment groups on a day to day basis. Statistical significance was determined by a p value <0.05.

Results

Preparation and characterization of micelles

Our overall goals were to prepare and characterize of CUR-, DOX-, and CUR + DOX-loaded micelles non-targeted and targeted with the GLUT1, evaluate their *in vitro* cytotoxicity against HCT-116 colorectal carcinoma cells and assess changes in anti-tumor activity with the combination treatment *in vivo*. CUR and/or DOX drug-loaded micelles were prepared by the thin film hydration method. At 5 mM concentration of PEG_{2000}-PE successfully incorporated DOX at a concentration of ~0.45 mg/ml (~3.2% w/w). CUR was also effectively encapsulated at a concentration of ~1.2 mg/ml (8.5% w/w). The same concentrations of both drugs were also achieved when co-loaded into a single micellar formulation. Loading efficiency was not affected by the addition of the targeting moiety. The micelles had sizes of $12.2 + 1.6$ nm and a zeta potential of -29.2 ± 0.91 mV for the non-targeted formulations. The GLUT1-targeted micelles had slightly larger size of $19.9 + 2.9$ nm and a zeta potential of -18.9 ± 1.1 mV.

A reverse phase HPLC method using a C18 column was developed to determine the drug concentrations in the micellar formulations simultaneously generated a clear separation between the CUR and DOX peaks. The loading efficiency was ~95% at the conditions used. Antibody activity after the attachment to the distal end of the PEG_{3400}-PE polymer was tested before proceeding with the experiments using the ELISA test with the GLUT1 blocking peptide as the antigen. The conjugation efficiency of the antibody was ~70% and the activity was completely retained after conjugation as determined by BCA and ELISA assays.

Cell viability assays

The *in vitro* cytotoxicity of the different micellar formulations was investigated using the HCT-116 cell line. Non-targeted empty and GLUT1-targeted PEG-PE micelles had minimal cytotoxic effects on the cells at the corresponding concentrations range used. The dose-response studies with CUR and DOX as a single agent are shown in Figure 1. The toxicity of the CUR or DOX-loaded micelles was equivalent to the toxicity observed with free drugs indicating that the micelles released the entrapped drug after internalization and their cargo retained its activity post encapsulation.

The GLUT1-targeted CUR loaded micelles had a significantly improved cytotoxicity versus the non-targeted formulation at various CUR concentrations. For example, after 48 h

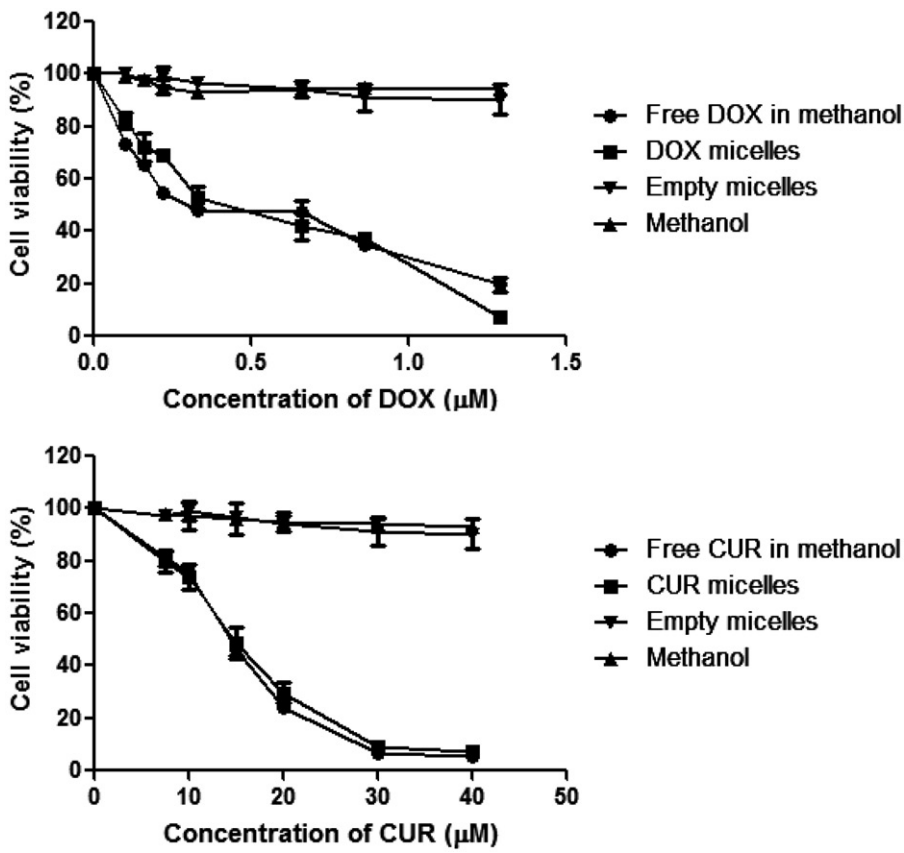

Figure 1. Cell viability of HCT-116 cells after 48 hrs of continuous incubation with free CUR/DOX or micellar CUR/DOX at various concentrations. Cell viability was determined using CellTiter Blue cell viability assay. Data shown are representative of three independent experiments performed in triplicate, mean ± SD.

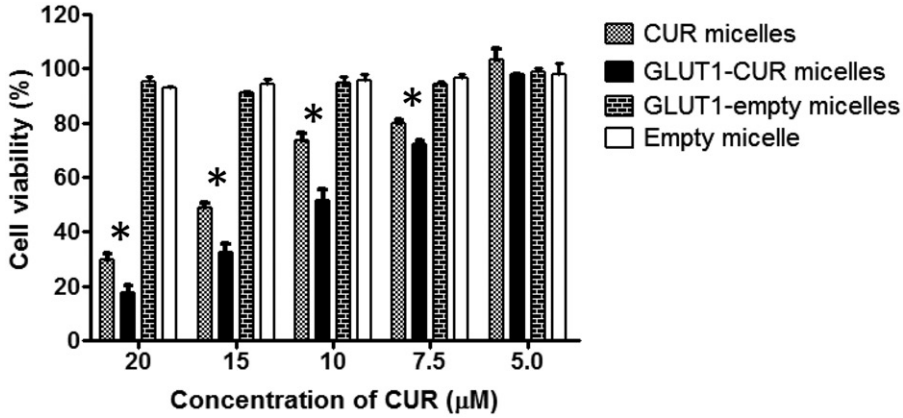

Figure 2. Cell viability of HCT-116 cells after 48 h of continuous incubation with empty, GLUT1-empty, CUR or GLUT1-targeted CUR micelles at various concentrations. Cell viability was determined using CellTiter Blue cell viability assay. Data shown are representative of three independent experiments performed in triplicate, mean ± SD $*p < 0.05$.

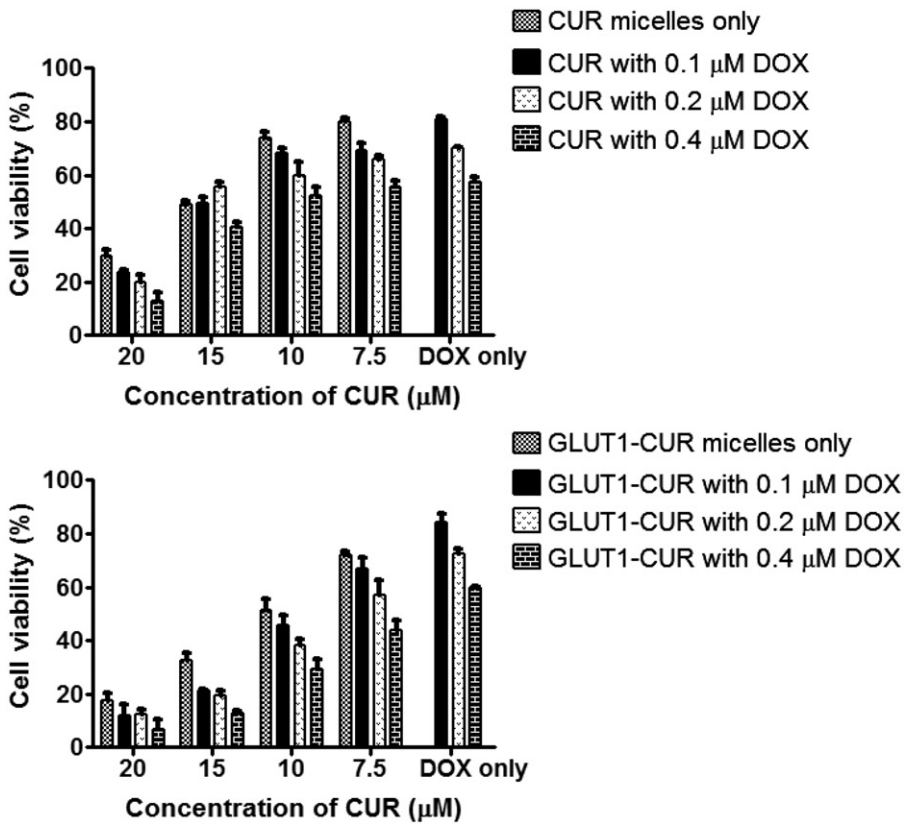

Figure 3. Cell viability of HCT-116 cells after 48 h of continuous incubation with combination micelles at various concentrations of CUR and DOX. Cell viability was determined using CellTiter Blue cell viability assay. Data shown are representative of three independent experiments performed in triplicate, mean ± SD.

of continuous incubation with 10 μM CUR, the formulation modified with GLUT1 killed ~50% of cells while the non-targeted treatment killed only 28%. This difference was statistically significant ($p < 0.05$) at all the concentrations tested in Figure 2. The IC_{50} of CUR micelles was ~15 μM while the GLUT1-CUR micelle IC_{50} was ~10 μM indicating a 30% greater improvement in toxicity.

CUR + DOX-loaded micelles decorated with GLUT1 had a robust killing effect even at low doses of DOX. The IC_{50} values of CUR with 0.1, 0.2, and 0.4 μM DOX micelles were ~13.7, 15.2, and 11.2 μM CUR, respectively. The addition of GLUT1 to the surface of the micelles decreased the IC_{50} values of CUR with 0.1, 0.2, and 0.4 μM DOX micelles to ~9.5, 8.3, and 6.8 μM, respectively. Using the targeted formulations, more than 80% of the HCT-116 cells were killed with a low dose of DOX (0.1 μM) in combination with 15 and 20 μM CUR (Figure 3).

Tumor inhibition study

Nude mice bearing ~250 mm^3 HCT-116 tumors were treated with 4 mg/kg CUR and 0.4 mg/kg DOX as a single treatment or in combination every 2 d till the end of the study. At the doses chosen, the formulations exhibited no toxicity *in vivo* indicated by a no significant decrease in body weight throughout the study. One way ANOVA from day 0 to 26 with Tukey's post-test showed that GLUT1-CUR and GLUT1-CUR + DOX were significantly different from the PBS control group. Also, GLUT1-CUR + DOX treatment was significantly different from the CUR group. Two way ANOVA analyses demonstrated that PBS was significantly different from: GLUT1-CUR beginning at day 14, CUR + DOX at day 20, and GLUT1-CUR + DOX at day 12 until the end the study. GLUT1-Empty is significantly different from GLUT1-CUR at day 26 and GLUT1-CUR + DOX at

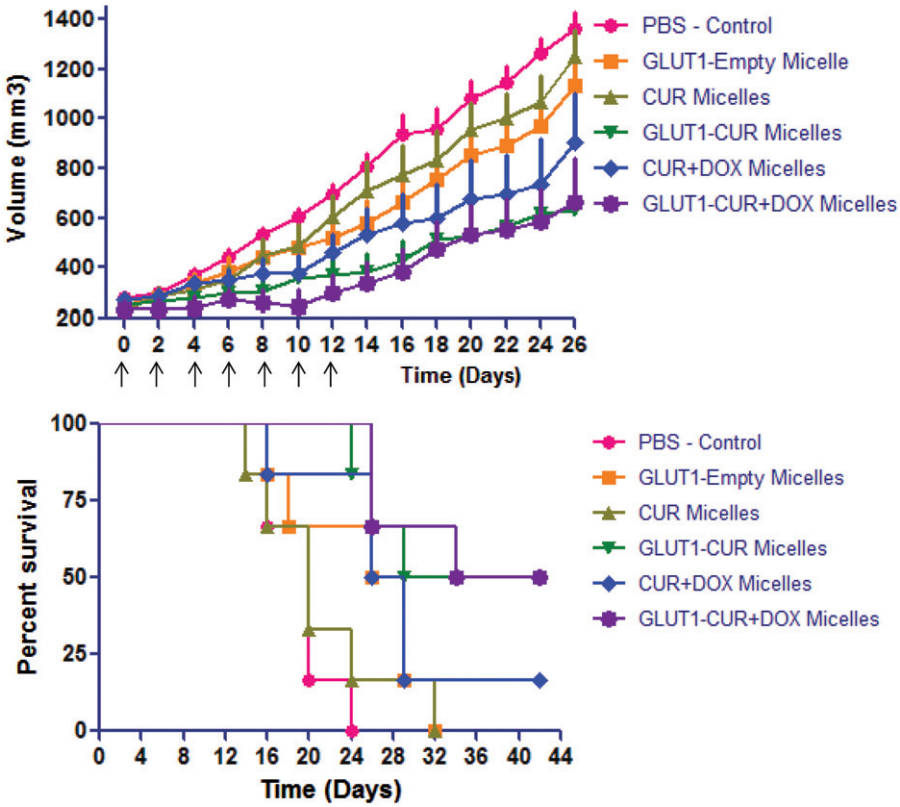

Figure 4. Tumor inhibition studies of various micellar formulations. Female nude (NU/NU) mice bearing ~250 mm^3 HCT-116 tumors were treated every 2 d starting at day 0 (7 total tail vein injections, arrows correspond to injection days) at a dose of 4 mg/kg CUR and 0.4 mg/kg DOX. $N = 6$ with SEM. Empty micelle dose was equivalent to the amount of lipid from the drug-loaded micelle groups. A – Tumor volume. B – Survival curve, survival was determined when the tumor reached 1000 mm^3, $*p < 0.05$.

day 24 and 26. CUR is significantly different from: GLUT1-CUR beginning at day 20 and GLUT1-CUR + DOX at day 14 until the end of the study.

CUR micelles at a dose of 4 mg/kg and GLUT1-empty micelles led to no significant tumor growth inhibition versus the PBS control group. DOX at a 0.4 mg/kg dose did not enhance the effect of CUR since no difference was observed between GLUT1-CUR + DOX and GLUT1-CUR groups. The CUR + DOX treatment group showed a trend towards better tumor inhibition than the CUR micelle treatment even though each alone had negligible effect on tumor growth. In the survival study, while all members of the PBS control group were non-viable by day 24, 50% of the GLUT1-CUR and GLUT1-CUR + DOX treatment groups remained alive at day 42 (Figure 4).

Discussion

In clinical settings, avoiding the use of an insufficient dose of a conventional chemotherapeutic agents is of the utmost importance in order to prevent tumors from acquiring resistance by upregulating NF-κB. To circumvent this phenomenon, clinicians are inclined to administer high doses of drug, which in turn lead to numerous undesirable side effects. The GLUT1-targeted CUR and DOX-loaded combination micelle could help minimize these side effects and at same time improve the treatment outcome. This could be achieved by increasing drug uptake at the target site by utilizing GLUT1 and at the same time preventing the cancer cells from acquiring drug resistance through the CUR-mediated inhibition of the NF-κB activity. In this study, we administered a suboptimal dose of DOX that was unable to confer resistance to the HCT-116 xenografts; this was evident since the GLUT1-CUR and GLUT1-CUR + DOX micelles significantly inhibited tumor growth at an equal level with both having a dramatic effect on survival. CUR-loaded micelles had negligible effects on tumor growth at the dose chosen. However, perhaps due to the increased internalization of targeted micelles via the GLUT1, a significant inhibition of tumor growth was observed by the GLUT1-CUR micelles. We also observed that GLUT1-empty micelles had a small suggestive effect on tumor growth, although with no statistically significant difference from the PBS-treated control group. Still, this trending may be attributed to the decrease in glucose uptake by blocking the GLUT1 transport protein. GLUT1 is not present in certain normal tissues but due to malignant transformation, it can be detected in various peri-necrotic regions of many human tumor types [34]. This difference in expression between normal tissue and tumors is sufficient to permit the targeting of the GLUT1 transporter with minimal side effects.

Here, we have demonstrated the effective use of GLUT1 as both a targeting moiety and apparently a tool to inhibit the GLUT1 transporter leading to a decrease in glucose uptake by colon cancer cells. We also established that these polymeric micelles used are suitable for delivering and shielding of CUR and DOX *in vivo*. These results justify further more detailed *in vivo* experiments and; therefore, we are currently investigating the efficacy of using higher doses of CUR and DOX that maximize the combinatory effect of both drugs.

Declaration of interest

This work was funded by Immix Co, in which Ilya M. Rachman, Sean Senn, and Vladimir P. Torchilin have interest.

References

1. Samanta AK, Huang HJ, Bast RC, Jr., Liao WS. Overexpression of MEKK3 confers resistance to apoptosis through activation of NFkappaB. J Biol Chem 2004;279:7576–83.
2. Shostak K, Chariot A. NF-κB, stem cells and breast cancer: the links get stronger. Breast Cancer Res 2011;13:214.
3. Voboril R, Weberova-Voborilova J. Constitutive NF-kappaB activity in colorectal cancer cells: impact on radiation-induced NF-kappaB activity, radiosensitivity, and apoptosis. Neoplasma 2006; 53:518–23.
4. Arlt A, Gehrz A, Muerkoster S, et al. Role of NF-kappaB and Akt/PI3K in the resistance of pancreatic carcinoma cell lines against gemcitabine-induced cell death. Oncogene 2003;22:3243–51.
5. Gupta SC, Sundaram C, Reuter S, Aggarwal BB. Inhibiting NF-κB activation by small molecules as a therapeutic strategy. Biochimica et Biophysica Acta (BBA) – Gene Regul Mech 2010;1799:775–87.
6. Huang S, DeGuzman A, Bucana CD, Fidler IJ. Nuclear factor-kappaB activity correlates with growth, angiogenesis, and metastasis of human melanoma cells in nude mice. Clin Cancer Res 2000;6:2573–81.
7. Yeh PY, Chuang S-E, Yeh K-H, et al. Involvement of nuclear transcription factor-κB in low-dose doxorubicin-induced drug resistance of cervical carcinoma cells. Biochem Pharmacol 2003; 66:25–33.
8. Anand P, Sundaram C, Jhurani S, et al. Curcumin and cancer: an ''old-age'' disease with an ''age-old'' solution. Cancer Lett 2008; 267:133–64.
9. Chaturvedi MM, Sung B, Yadav VR, et al. NF-kappaB addiction and its role in cancer: 'one size does not fit all'. Oncogene 2011;30: 1615–30.
10. Epelbaum R, Schaffer M, Vizel B, et al. Curcumin and gemcitabine in patients with advanced pancreatic cancer. Nutr Cancer 2010;62: 1137–41.
11. Tsai Y-M, Jan W-C, Chien C-F, et al. Optimised nano-formulation on the bioavailability of hydrophobic polyphenol, curcumin, in freely-moving rats. Food Chem 2011;127:918–25.
12. Shaikh J, Ankola DD, Beniwal V, et al. Nanoparticle encapsulation improves oral bioavailability of curcumin by at least 9-fold when compared to curcumin administered with piperine as absorption enhancer. Eur J Pharm Sci 2009;37:223–30.
13. Sun J, Bi C, Chan HM, et al. Curcumin-loaded solid lipid nanoparticles have prolonged *in vitro* antitumour activity, cellular uptake and improved *in vivo* bioavailability. Colloids Surf B: Biointerfaces 2013;111:367–75.
14. Kakkar V, Muppu SK, Chopra K, Kaur IP. Curcumin loaded solid lipid nanoparticles: an efficient formulation approach for cerebral ischemic reperfusion injury in rats. Eur J Pharm Biopharm 2013. [Epub ahead of print]. http://dx.doi.org/10.1016/j.ejpb.2013.02.005.
15. Gangwar RK, Dhumale VA, Kumari D, et al. Conjugation of curcumin with PVP capped gold nanoparticles for improving bioavailability. Mat Sci Eng: C 2012;32:2659–63.
16. Akhtar F, Rizvi MMA, Kar SK. Oral delivery of curcumin bound to chitosan nanoparticles cured *Plasmodium yoelii* infected mice. Biotechnol Adv 2012;30:310–20.
17. Sahu A, Bora U, Kasoju N, Goswami P. Synthesis of novel biodegradable and self-assembling methoxy poly(ethylene glycol)–palmitate nanocarrier for curcumin delivery to cancer cells. Acta Biomater 2008;4:1752–61.
18. Suwannateep N, Banlunara W, Wanichwecharungruang SP, et al. Mucoadhesive curcumin nanospheres: biological activity, adhesion to stomach mucosa and release of curcumin into the circulation. J Control Release 2011;151:176–82.
19. Kirpotin DB, Drummond DC, Shao Y, et al. Antibody targeting of long-circulating lipidic nanoparticles does not increase tumor localization but does increase internalization in animal models. Cancer Res 2006;66:6732–40.
20. Mueckler M, Thorens B. The SLC2 (GLUT) family of membrane transporters. Mol Aspects Med 2013;34:121–38.
21. Macheda ML, Rogers S, Best JD. Molecular and cellular regulation of glucose transporter (GLUT) proteins in cancer. J Cell Physiol 2005;202:654–62.
22. Yamamoto T, Seino Y, Fukumoto H, et al. Over-expression of facilitative glucose transporter genes in human cancer. Biochem Biophys Res Commun 1990;170:223–30.
23. Boado RJ, Black KL, Pardridge WM. Gene expression of GLUT3 and GLUT1 glucose transporters in human brain tumors. Mol Brain Res 1994;27:51–7.
24. Brown RS, Wahl RL. Overexpression of Glut-1 glucose transporter in human breast cancer. An immunohistochemical study. Cancer 1993;72:2979–85.
25. Vander Heiden MG, Cantley LC, Thompson CB. Understanding the Warburg effect: the metabolic requirements of cell proliferation. Science 2009;324:1029–33.
26. Cairns RA, Harris IS, Mak TW. Regulation of cancer cell metabolism. Nat Rev Cancer 2011;11:85–95.
27. Gu J, Yamamoto H, Fukunaga H, et al. Correlation of GLUT-1 overexpression, tumor size, and depth of invasion with 18F-2-fluoro-2-deoxy-D-glucose uptake by positron emission tomography in colorectal cancer. Dig Dis Sci 2006;51:2198–205.
28. Squires MS, Feltell RE, Wallis NG, et al. Biological characterization of AT7519, a small-molecule inhibitor of cyclin-dependent kinases, in human tumor cell lines. Mol Cancer Ther 2009;8: 324–32.
29. Evans A, Bates V, Troy H, et al. Glut-1 as a therapeutic target: increased chemoresistance and HIF-1-independent link with cell turnover is revealed through COMPARE analysis and metabolomic studies. Cancer Chemother Pharmacol 2008;61:377–93.
30. Szablewski L. Expression of glucose transporters in cancers. Biochimica et Biophysica Acta (BBA) - Rev Cancer 2013;1835: 164–9.
31. Cantuaria G, Magalhaes A, Penalver M, et al. Expression of GLUT-1 glucose transporter in borderline and malignant epithelial tumors of the ovary. Gynecol Oncol 2000;79:33–7.
32. Sung JY, Kim GY, Lim SJ, et al. Expression of the GLUT1 glucose transporter and p53 in carcinomas of the pancreatobiliary tract. Pathol Res Pract 2010;206:24–9.
33. Firth JD. Hypoxia and mitochondrial inhibitors regulate expression of glucose transporter-1 via distinct Cis-acting sequences. J Biol Chem 1995;270:29083–9.
34. Airley R, Evans A, Mobasheri A, Hewitt SM. Glucose transporter Glut-1 is detectable in peri-necrotic regions in many human tumor types but not normal tissues: study using tissue microarrays. Ann Anat 2010;192:133–8.